

Constraints on Axion-Like Particles from Ultra-High-Energy Observations of 3HWC J1908+063 with HAWC

R. Alfaro^{a,*} C. Alvarez^b A. Andrés^c E. Anita-Rangel^c M. Araya^d
 J.C. Arteaga-Velázquez^e D. Avila Rojas^c H.A. Ayala Solares^f
 R. Babu^g P. Bangale^f E. Belmont-Moreno^a A. Bernal^c
 K.S. Caballero-Mora^b T. Capistrán^c A. Carramiñana^h F. Carreón^c
 S. Casanovaⁱ U. Cotti^e J. Cotzomi^j E. De la Fuente^k P. Desiatil^l
 N. Di Lalla^m R. Diaz Hernandez^h M.A. DuVernois^l
 J.C. Díaz-Vélez^l T. Ergin^g C. Espinoza^a N. Fraija^c S. Fraija^c
 J.A. García-Gonzálezⁿ F. Garfias^c N. Ghosh^o A. Gonzalez Muñoz^a
 M.M. González^c J.A. González^e J.A. Goodman^p J. Gyeong^q
 J.P. Harding^r S. Hernández-Cadena^{ab,*} I. Herzog^g D. Huang^p
 F. Hueyotl-Zahuantitla^b A. Iriarte^c S. Kaufmann^s D. Kieda^t
 A. Lara^u W.H. Lee^c J. Lee^v H. León Vargas^a A.L. Longinotti^c
 G. Luis-Raya^s K. Malone^r O. Martinez^j J. Martínez-Castro^w
 H. Martínez-Huerta^x J.A. Matthews^y P. Miranda-Romagnoli^z
 P.E. Mirón-Enriquez^c J.A. Morales-Soto^e E. Moreno^j M. Mostafá^f
 M. Najafi^o A. Nayerhodaⁱ L. Nellen^{aa} M.U. Nisa^g
 R. Noriega-Papaqui^z N. Omodei^m E. Ponce^j Y. Pérez Araujo^a
 E.G. Pérez-Pérez^s A. Pratts^{a,*} C.D. Rho^q A. Rodriguez Parra^e
 D. Rosa-González^h M. Roth^r A. Sandoval^a M. Schneider^p
 J. Serna-Franco^a A.J. Smith^p Y. Son^v R.W. Springer^t O. Tibolla^s
 K. Tollefson^g I. Torres^h R. Torres-Escobedo^{ab} E. Varela^j
 L. Villaseñor^j X. Wang^{ac} Z. Wang^{ac} I.J. Watson^v H. Wu^l S. Yu^{ad}
 X. Zhangⁱ H. Zhou^{ab} C. de León^e

^aInstituto de Física, Universidad Nacional Autónoma de México, Ciudad de México, México

^bUniversidad Autónoma de Chiapas, Tuxtla Gutiérrez, Chiapas, México

^cInstituto de Astronomía, Universidad Nacional Autónoma de México, Ciudad de México, México

^dUniversidad de Costa Rica, San José 2060, Costa Rica

^eUniversidad Michoacana de San Nicolás de Hidalgo, Morelia, México

^fTemple University, Department of Physics, 1925 N. 12th Street, Philadelphia, PA 19122, USA

^gDepartment of Physics and Astronomy, Michigan State University, East Lansing, MI, USA

^hInstituto Nacional de Astrofísica, Óptica y Electrónica, 72000 Puebla, México

ⁱInstitute of Nuclear Physics Polish Academy of Sciences, PL-31342 Krakow, Poland

^jFacultad de Ciencias Físico Matemáticas, Benemérita Universidad Autónoma de Puebla, Puebla, México

^kDepartamento de Física, Centro Universitario de Ciencias Exactas e Ingenierías, Universidad de Guadalajara, Guadalajara, México

^lDept. of Physics and Wisconsin IceCube Particle Astrophysics Center, University of Wisconsin-Madison, Madison, WI, USA

^mDepartment of Physics, Stanford University, Stanford, CA 94305-4060, USA

ⁿTecnológico de Monterrey, Especialidad Licenciatura Ciencias Astronómicas, Ciudad Guadalupe, México

^wCentro de Investigación en Computación, Instituto Politécnico Nacional, México City, México

^xUniversidad de Monterrey, San Pedro Garza García, Nuevo León, México

^yDept of Physics and Astronomy, University of New Mexico, Albuquerque, NM, USA

^zUniversidad Autónoma del Estado de Hidalgo, Pachuca, México

^{aa}Instituto de Ciencias Nucleares, Universidad Nacional Autónoma de México, Ciudad de México, México

^{ab}Tsung-Dao Lee Institute & School of Physics and Astronomy, Shanghai Jiao Tong University, 800 Dongchuan Rd, Shanghai 200240, China

^{ac}Department of Physics, Missouri University of Science and Technology, Rolla, MO, USA

^{ad}Department of Physics, Pennsylvania State University, University Park, PA, USA

E-mail: yoba_m_t_a@ciencias.unam.mx, shkdna@sjtu.edu.cn,
ruben@fisica.unam.mx

Abstract. Axion-like particles (ALPs) are hypothetical particles and compelling candidates for cold dark matter. Their existence could be probed through their conversions into photons in the presence of magnetic fields. In this work, we explore the effect of these photon-ALP conversions by searching for an attenuation in the observed gamma ray spectra of galactic sources that emit at energies of hundreds of TeV. We analyze data from the High-Altitude Water Cherenkov (HAWC) Observatory for the source 3HWC J1908+063. No evidence of photon-ALP conversions was found, and we set constraints on the ALP parameter space. Specifically, we derive exclusion limits for ALPs with masses in the range 10^{-8} eV $\leq m_a \leq 10^{-6}$ eV and photon-ALP couplings in the range 10^{-12} GeV $^{-1} \leq g_{a\gamma} \leq 10^{-10}$ GeV $^{-1}$, based on HAWC observations.

Keywords: axions, gamma ray experiments, dark matter experiments

Contents

1	Introduction	1
2	Axion-Like Particles	2
3	Source selection and data	4
4	Method	6
5	Results	7
5.1	Null TS Distribution	7
5.2	Exclusion Region	8
6	Conclusions	10

1 Introduction

Axions are hypothetical particles proposed as a solution to the strong CP problem in quantum chromodynamics (QCD). This problem concerns the observed conservation of charge–parity (CP) symmetry, even though QCD permits CP violation through a nonzero θ -term. One of the most prominent theoretical resolutions is the Peccei–Quinn mechanism, which introduces a new global $U(1)$ symmetry whose spontaneous breaking predicts the existence of a light pseudoscalar particle known as the axion [1]. The Peccei–Quinn idea can be extended to broader theoretical frameworks, including string theory, where it naturally predicts a family of particles known as axion-like particles (ALPs) [2]. Both axions and ALPs are compelling candidates for dark matter due to their potential to exist in a non-relativistic (cold) state, moving at low velocities as predicted by the Λ CDM cosmological model [3, 4].

Unlike heavy dark matter candidates such as weakly interacting massive particles (WIMPs), ALPs are characterized by their very low mass, ranging from a few GeV down to 10^{-20} eV, which makes their direct detection particularly challenging. However, ALPs possess a unique property: their coupling to electromagnetism. This coupling enables photon-ALP conversions in the presence of magnetic fields, with the conversion probability depending on factors such as energy, magnetic field strength, and propagation distance. Due to this, astrophysical sources represent a significant opportunity for the study of ALPs, as they provide the conditions under which these conversions could occur. In particular, sources that emit at UHE have been of interest because an increase in the photon energy also increases the probability of photon-ALP conversion, which could manifest as distortions in the observed gamma-ray spectrum [5–14].

Previous investigations, such as those using Fermi-LAT [15], H.E.S.S [16] and High-Altitude Water Cherenkov Observatory (HAWC) public data [17], have focused on distant emission sources, particularly active galaxies like PKS 2155-304 and PG 1553+113, to ensure the presence of these photon-ALP oscillations. However, these studies suffer from systematic uncertainties arising from modeling and limited knowledge of several parameters, such as the extragalactic background light (EBL), magnetic fields, and the intrinsic spectrum [18].

Advances in instrumentation capable of detecting ultra-high energies [19] have made it possible to study closer galactic sources emitting at tens or hundreds of TeV. Such sources,

including pulsar wind nebulae, supernova remnants, and TeV halos, have been reported by HAWC Observatory [20], presenting new opportunities to explore photon-ALP conversions in galactic environments.

Studying galactic sources offers distinct advantages over extragalactic ones, including the avoidance of EBL effects and more accurate modeling of the galactic magnetic field, reducing systematic uncertainties significantly. These factors enable a more reliable interpretation of the high-energy spectra from galactic sources, as uncertainties related to photon propagation through poorly known intergalactic media are minimized [21–24].

The effect of EBL absorption is negligible for galactic sources at energies below PeV due to the relatively short distance between the source and Earth. Additionally, when modeling the magnetic field for a galactic source, only the Milky Way’s magnetic field enters the calculations of ALP conversions. However, there are still some important considerations when studying galactic sources. The probability of photon-ALP conversion is dependent on the distance traveled by the photon within the magnetic field, which is considerably reduced in the galactic case compared to the extragalactic scenario. To compensate for this, other parameters in the conversion probability must be increased. This can be achieved by employing this using ultra-high-energy (UHE) photons.

This paper is organized as follows, in Section 2 we present details about ALPs and their mixing with photons, including the conversion probability that is the main observable when considering the effect of oscillations in the photon spectrum of galactic sources. In Section 3, we present the source used in this analysis. Section 4 is dedicated to explaining the analysis methodology used in our work, focusing on the issue of non-nested hypotheses and the approach we use to derive non-biased upper limits. Finally, in Sections 5 and 6 we discuss our results and present our conclusions. In this work, we refer to UHE photons as those detected above tens of TeV and up to a few hundred TeV. Observatories like HAWC, which can detect photons above tens of TeV, are well suited for searching for ALP-induced spectral anomalies, as conversion probabilities become non-negligible in this energy range.

2 Axion-Like Particles

ALPs can oscillate into photons in the presence of magnetic fields, an effect expected to be particularly relevant in high-energy astrophysics. The dynamics of ALPs are governed by the Lagrangian [2]:

$$\mathcal{L}_{\text{ALP}} = \frac{1}{2} (\partial_\mu a \partial^\mu a - m_a^2 a^2) + \frac{1}{4f_a} a F_{\mu\nu} \tilde{F}^{\mu\nu}, \quad (2.1)$$

where a represents the ALP field, m_a is the ALP mass, $F_{\mu\nu}$ denotes the Faraday tensor, $\tilde{F}^{\mu\nu}$ is its dual, and f_a is the ALP decay constant.

The interaction between ALPs and the electromagnetic field is described by:

$$\mathcal{L}_{a\gamma} = \frac{1}{4f_a} a F_{\mu\nu} \tilde{F}^{\mu\nu} = a g_{a\gamma} \vec{E} \cdot \vec{B}, \quad (2.2)$$

where $g_{a\gamma} = \frac{1}{f_a}$ is the photon-ALP coupling constant, and \vec{E} and \vec{B} are the electric and magnetic fields, respectively.

In the presence of an external magnetic field \vec{B} , ALPs and photons can mix, leading to oscillations between these states. This interaction is described by a mixing matrix \mathcal{M} , which encapsulates the equations of motion for the coupled system. Assuming a constant transverse

magnetic field aligned with the z -axis, the mixing matrix for the photon field component A_{\parallel} (parallel to \vec{B}) and the ALP field a can be expressed in Fourier space as:

$$\mathcal{M} = \begin{pmatrix} \Delta_{\parallel} & \Delta_{a\gamma} \\ \Delta_{a\gamma} & \Delta_a \end{pmatrix}, \quad (2.3)$$

where Δ_{\parallel} represents the effective mass term for photons in the medium, $\Delta_{a\gamma} = g_{a\gamma}B$ is the mixing term that depends on the coupling constant $g_{a\gamma}$ and the magnetic field strength B , and $\Delta_a = \frac{m_a^2}{2E_{\gamma}}$ is the term related to the ALP, with m_a being the ALP mass and E_{γ} the photon energy.

To account for the evolution of the quantum state along the direction of propagation, we use the density matrix formalism. The density matrix $\rho(z)$ describes the quantum state of the system and evolves according to the von Neumann-like equation:

$$i \frac{d\rho}{dz} = [\rho, \mathcal{M}]. \quad (2.4)$$

The solution to this equation can be expressed using the transfer matrix $\mathcal{T}(z, 0; E_{\gamma})$:

$$\rho(z) = \mathcal{T}(z, 0; E_{\gamma})\rho(0)\mathcal{T}^{\dagger}(z, 0; E_{\gamma}), \quad (2.5)$$

where the transfer matrix $\mathcal{T}(z, 0; E_{\gamma})$ propagates the initial state $\rho(0)$ over the distance z . This matrix is constructed by considering small steps dz in the z -direction, assuming that the magnetic field is constant over each step:

$$\mathcal{T}(z_N, z_1; E_{\gamma}) = \prod_{i=1}^N \mathcal{T}(z_{i+1}, z_i; E_{\gamma}). \quad (2.6)$$

The photon survival probability, $P_{\gamma\gamma}$, is obtained by tracing the density matrix projected onto the photon states:

$$P_{\gamma\gamma} = \text{Tr} \left((\rho_{11} + \rho_{22}) \mathcal{T}(z_N, z_1; E_{\gamma}) \rho(0) \mathcal{T}^{\dagger}(z_N, z_1; E_{\gamma}) \right), \quad (2.7)$$

here, $\rho_{11} = \text{diag}(1, 0, 0)$ and $\rho_{22} = \text{diag}(0, 1, 0)$, corresponding to the photon components. This formulation accounts for both the oscillations induced by the magnetic field and variations along the line of sight, allowing for a more precise modeling of photon-ALP conversions and the subsequent evolution of the system.

The photon survival probability can be expressed as:

$$P_{\gamma\gamma} = (1 - P_{\gamma \rightarrow a}), \quad (2.8)$$

where $P_{\gamma \rightarrow a}$ is the photon-ALP conversion probability.

In the case of a homogeneous magnetic field B the probability is given by:

$$P_{\gamma \rightarrow a}(E_{\gamma}) = \left(1 + \frac{E_c^2}{E_{\gamma}^2} \right)^{-1} \sin^2 \left(\frac{g_{a\gamma} B_T L}{2} \sqrt{1 + \frac{E_c^2}{E_{\gamma}^2}} \right), \quad (2.9)$$

where B_T is the transverse magnetic field relative to the photon's direction of motion, L is the distance traveled within the magnetic field, $g_{a\gamma}$ is the coupling constant, and E_c is the critical energy, a reference energy above which the interaction (mixing) of the photon beam and ALPs becomes significant and can be expressed as:

$$E_c = \frac{|m_a^2 - \omega_{\text{pl}}^2|}{2g_{a\gamma}B_T}, \quad (2.10)$$

with $\omega_{\text{pl}}^2 = \frac{4\pi\alpha n_e}{m_e}$, the plasma frequency of the medium, n_e the electron density, m_e the electron mass, and α the fine structure constant.

The observed photon flux on Earth from a source, taking into account photon-ALP conversions, is:

$$\frac{d\phi}{dE_\gamma} = (1 - P_{\gamma \rightarrow a}) f_{\text{att}} \left. \frac{d\phi}{dE_\gamma} \right|_{\text{source}}. \quad (2.11)$$

The intrinsic spectrum is denoted as $\left. \frac{d\phi}{dE_\gamma} \right|_{\text{source}}$, and refers to the spectrum emitted at the source. $P_{\gamma \rightarrow a}$ is the photon-ALP conversion probability, and f_{att} is a factor that accounts for the attenuation of the flux due to interactions with the EBL and from other effects like local photon fields. For galactic sources, the attenuation factor f_{att} is ≈ 1 due to the proximity of the source to the observer and the energy of the photons. Therefore, the conversion probability $P_{\gamma \rightarrow a}$ is the most relevant factor in the potential distortion of the intrinsic flux.

3 Source selection and data

The HAWC Observatory, located at an altitude of 4100m on the slopes of the Sierra Negra volcano in Mexico, is designed to observe gamma rays in the energy range from ~ 1 TeV up to several hundred TeV. HAWC uses the water cherenkov detection technique, consisting of 300 water cherenkov detectors (WCDs), each instrumented with four photomultiplier tubes that measure the cherenkov light produced by secondary particles in extensive air showers. HAWC operates continuously, covering about two-thirds of the sky every day, and has been taking data since 2015 [25]. The data used in this work correspond to Pass 5 reconstruction which comprises several years of operation and is binned in different energy estimators to cover a wide dynamic range [26]. In addition to Galactic and extragalactic source studies, HAWC has performed a variety of dark matter searches. Relevant details can be found in [27–30] and references therein.

The HAWC Collaboration has reported observations of UHE sources in the 3HWC catalog [20], where multiple galactic sources show emission at energies above 56 TeV. We focus on these sources because the probability of photon-ALP conversion increases with energy, making UHE sources particularly valuable for such studies.

In this work, we focus on the source 3HWC J1908+063, which is one of the brightest galactic sources observed by HAWC at energies exceeding 100 TeV [31]. The spectrum of 3HWC J1908+063 has been studied by HAWC and other TeV gamma-ray observatories [32–34]; and it provides an excellent opportunity to search for potential ALP-induced effects.

In order to illustrate and support the claim that UHE gamma rays are ideal for probing ALP-induced effects, it is useful to look at the predicted photon-ALP conversion probabilities for typical galactic parameters (magnetic field strength and distances) in the TeV range. Such a probability curve typically rises with energy, providing a strong motivation to analyze UHE gamma-ray data. Figure 1 shows the variation of the conversion probability for a specific ALP candidate and its potential impact on the source's gamma-ray spectrum detected by HAWC, particularly at high energies.

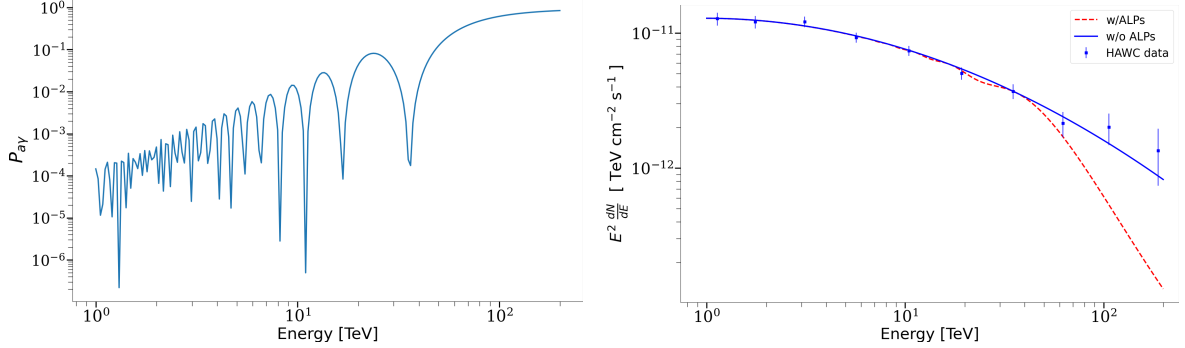


Figure 1: Left panel: Photon-ALP conversion probability as a function of energy for an ALP candidate with parameters $m_a = 9 \times 10^{-7}$ eV and $g_{a\gamma} = 8 \times 10^{-11}$ GeV $^{-1}$. Right panel: Expected effect of this candidate on the UHE spectrum of the source and assuming a distance to the earth of 3.2 kpc (red dotted line) compared with the log-parabola fit reported by HAWC without ALPs hypothesis (blue line).

The astrophysical parameters associated with the source, such as the distance to Earth and the magnetic field strength, are crucial when calculating the photon survival probability. The source 3HWC J1909+063 was initially reported by the Milagro observatory and later by H.E.S.S. It has been associated with PSR J1907+062 and SNR G40.5–0.5 [35, 36]. Multi-TeV emission can be explained by leptonic processes in the pulsar wind nebula (PWN), with an estimated distance of 3.2 kpc based on dispersion measure (DM) data from Arecibo Observatory. However, multi-TeV emission above 10 TeV can also be explained using leptohadronic models connected to the SNR, which has been reported to lie between 3–3.5 kpc and 8–9.5 kpc [37]. This is also one of the motivations for selecting this source: beyond its UHE emission, its distance contributes to enhancing the photon-ALP conversion probability.

Regarding the magnetic field, there are various studies of the Galactic magnetic field. For our analysis, we rely on the model from [38], which considers distinct components for the disk, halo, and poloidal regions of the Milky Way (MW). However, since the source is located in the Galactic plane, we can assume that the disc is the dominant component and neglect other contributions. As a first approximation, we assume a homogeneous magnetic field of 3 μ G, which is consistent with values reported for the solar neighborhood.

To verify that this approximation is valid, we use the `GammaALPs` [39] code to calculate the photon survival probability in two different scenarios. In the first scenario, we use the full model from [38], while in the second, we assume a simpler, homogeneous magnetic field along the line of sight between 3HWC J1908+063 and Earth. We find that both scenarios yield consistent results, at least for the range of mass and coupling constant of interest. This result reveals an additional advantage of using Galactic sources: it is not always necessary to employ the complete magnetic field model, thereby reducing the computational effort.

Our results are also consistent with other studies that assume the MW magnetic field can be described by both a regular and a turbulent component, and that at distances of a few kpc, only the regular and homogeneous component is dominant. Taking the previous points into account, in this study we examine several scenarios. Our baseline setup assumes a distance of 3.2 kpc (the distance associated with the PWN) and a magnetic field of 3 μ G. We also explore scenarios with distances of 5 kpc and 8 kpc, which could be consistent with the SNR association. Additionally, to illustrate the magnetic field's impact, we include a

scenario with a $1 \mu\text{G}$ field strength, which underscores the importance of the magnetic field in our results.

4 Method

To investigate the possible effect induced by photon-ALP conversions on the spectrum of the source 3HWC J1908+063, we compare two spectral models to describe the flux detected by HAWC: a log-parabola model without ALP conversions (null hypothesis), and a log-parabola model including the effects of ALP-photon conversions(alternative hypothesis). The choice of using a log-parabola model for the null hypothesis is motivated by its better fit to the data at energies above 100 TeV, and it is also consistent with the spectrum reported in [37]. That means that in 2.11,

$$\frac{d\phi}{dE_\gamma} \Big|_{\text{source}} = K \left(\frac{E}{E_0} \right)^{-\alpha - \beta \log \left(\frac{E}{E_0} \right)}, \quad (4.1)$$

where E_0 represents the pivot energy and for the null hypothesis $P_{\gamma \rightarrow a} = 0$. For each model, we obtained the best-fit parameters by fitting the observed data. We then used the likelihood ratio as a test statistic (TS) to decide which model better describes the data and to search for evidence of photon-ALP conversions.

For the alternative hypothesis, which includes ALP-photon conversions, we determined the optimal spectral parameters, $\{K, \alpha, \beta, m_a, g_{a\gamma}\}$, by fitting the model described by Eq. 2.11 and the log-parabola model 4.1.

To define the exclusion region, we utilized the test statistic (TS), calculated as the logarithmic likelihood (LL) ratio:

$$TS = -2 \left(\ln \mathcal{L}(\theta_0; m_a, g_{a\gamma} = 0) - \ln \mathcal{L}(\hat{\theta}_{m_a, g_{a\gamma}}) \right), \quad (4.2)$$

where $\ln \mathcal{L}(\theta_0; m_a, g_{a\gamma} = 0)$ represents the LL under the null hypothesis (log-parabola; no ALPs), and $\ln \mathcal{L}(\hat{\theta}_{m_a, g_{a\gamma}})$ is the LL under the alternative hypothesis (ALPs; log-parabola + ALPs) for given values of m_a and $g_{a\gamma}$.

The analysis was conducted using the Multi-Mission Maximum Likelihood Framework (3ML) in conjunction with the HAWC Accelerated Likelihood plugin (HAL) [26]. Additionally, the construction of the final exclusion regions in the $(m_a, g_{a\gamma})$ space was performed using the ZEBRA software, which allows a systematic scan over the parameter grid. For each fit, we recorded the LL values for the tested models (log-parabola or log-parabola + ALPs), the LL of the background-only (no source) hypothesis, and the corresponding TS. The LL values for the alternative hypothesis were calculated over a grid of 25×25 points for m_a and $g_{a\gamma}$ in the region $[10^{-8}, 10^{-5}] \text{ eV} \times [10^{-12}, 10^{-10}] \text{ GeV}^{-1}$ respectively. To complement this, we performed an analysis over a larger region of the sky, including nearby sources, to ensure that the intrinsic spectrum obtained for our source was not affected in any way by surrounding emission.

Due to the presence of non-linear dependencies inherent in ALP-photon conversion probabilities and dependencies on other quantities, such as magnetic field strength and electron density, Wilks' theorem does not hold in this case. Furthermore, the assumption that the null hypothesis (log-parabola) and the alternative hypothesis (including ALP-photon conversions) are nested hypotheses is generally invalid. This is because when the ALP mass is zero, it results in a degenerate solution where the coupling constant $g_{a\gamma}$ can take any value. Previous studies on the impact of ALP-photon conversion on the spectra of galactic and

extragalactic sources [15, 21, 40, 41] have shown that using classical quantiles (2.71 or 5.99) can lead to under coverage issues in the confidence intervals derived, as the statistical test based on the likelihood does not follow a χ^2 distribution with degrees of freedom equal to the difference in parameters between the null and alternative hypotheses.

Following the methodology outlined in [21], we generated a set of pseudo-experiments by fluctuating the expected model counts for the gamma-ray flux, assuming the null hypothesis (log-parabola). For each PE, we computed likelihoods for the null and the alternative and obtained the TS for the inclusion of the ALP hypothesis against the log-parabola spectrum model. All spectral parameters were allowed to vary freely in each fit. We computed the TS for a total of 300 pseudo-experiments and checked whether the resulting distribution could be described by a χ^2 distribution. For this distribution, we estimated a new TS threshold to set a 95% confidence level (C.L.) upper limit for the parameter space $(m_a, g_{a\gamma})$. This distribution enables an accurate estimation of the significance of a (non)-detection.

5 Results

We present the results obtained from our search for evidence of photon-ALP conversions at TeV energies. First, we present the TS distribution obtained from our pseudo-experiments. Then, as we do not find evidence of ALP-induced effects in the spectrum of 3HWC J1908+063, we estimate the exclusion region in the ALP parameter space.

5.1 Null TS Distribution

We computed the TS for the ALP hypothesis relative to the null hypothesis. The resulting normalized TS distribution is shown in Figure 2.

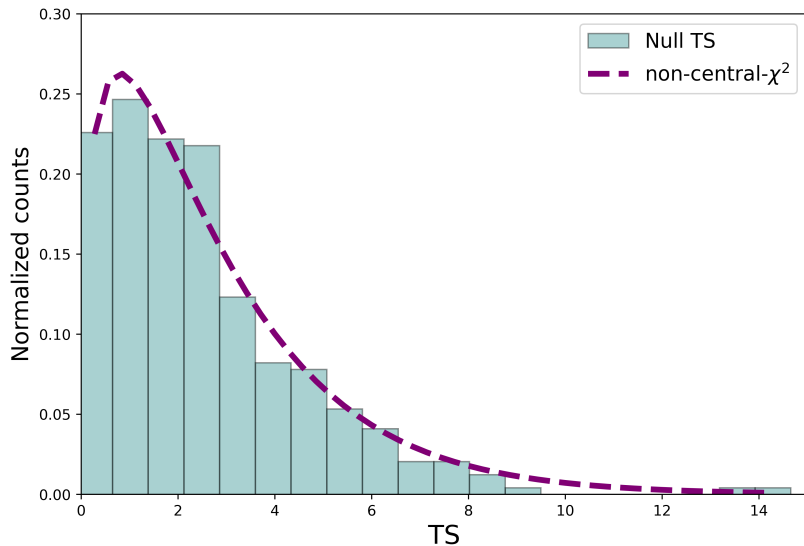


Figure 2: Best fit to the null TS distribution using a χ^2 distribution with effective degrees of freedom.

We fitted a χ^2 function to this distribution and found that the distribution is well described by a χ^2 distribution with 2.8 ± 0.1 effective degrees of freedom. This differs from

the expected result of a χ^2 distribution with two degrees of freedom. As previously discussed in Section 4, this deviation arises due to the non-applicability of Wilks' theorem and the non-nested nature of the hypotheses. Using the best-fit parameters of the empirical χ^2 distribution derived from the pseudo-experiments, we determined that the test statistic (TS) value corresponding to the 95% confidence level is 7.5. This value was used to establish the exclusion region in the parameter space $(m_a, g_{a\gamma})$. Additionally, the TS obtained from the observations of J1908+063 was 4.39, corresponding to an approximately 80% C.L, indicating that the observed data is consistent with the null hypothesis.. Then, the observed flux of J1908+063 is well described by a log-parabola spectrum, with no statistically significant indication of ALP-induced effects.

5.2 Exclusion Region

Using the results obtained from the mapping of the likelihood ratio outlined in Section 4 and the results from the pseudo-experiments 5.1, we determined the exclusion region by applying the ΔTS criteria with a threshold value of 7.5 at the 95% C.L. The resulting exclusion region is shown in Figure 3

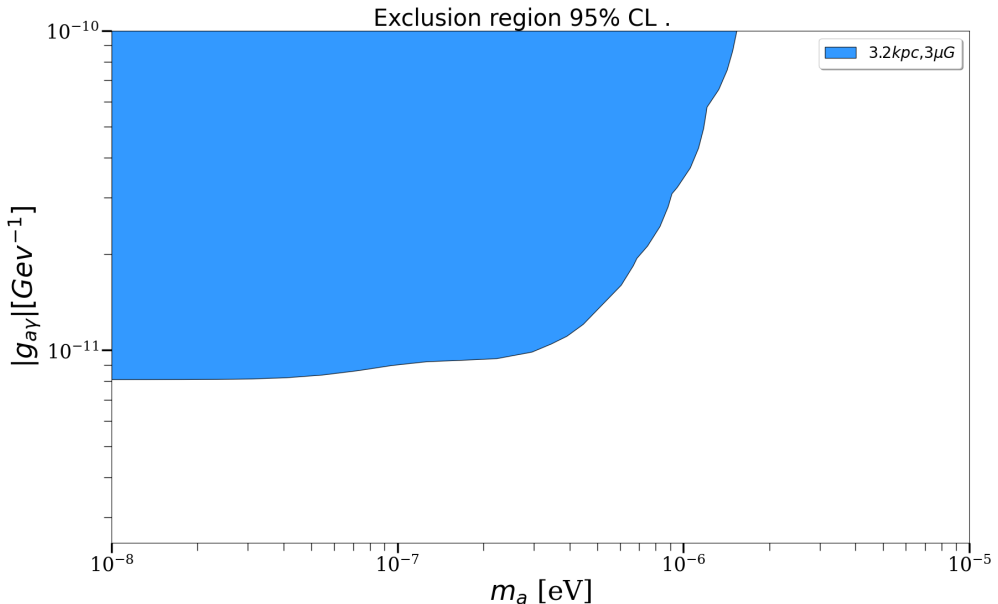


Figure 3: Exclusion region obtained for m_a and $g_{a\gamma}$ based on observations of the galactic source J1908+063, using HAWC data.

To assess the impact of varying parameters on the exclusion region, we examined how changes in distance and magnetic field strength affect the results. The values used for the magnetic field and distance are summarized in Table 1. The comparison between exclusion regions under different assumptions is shown in Figure 4, illustrating that for a smaller value of the specified field strength, the exclusion region is reduced. This is consistent with the fact that the conversion probability is proportional to B_T^2 . A similar effect is observed when varying the distance to the source; a larger distance increases the conversion probability due to the longer path length in the magnetic field, expanding the exclusion region.

It can also be observed that the expansion of the exclusion region occurs almost entirely in terms of the coupling constant rather than the mass. To understand this, it is helpful to

recall the expression for the critical energy, eq 2.10, which depends inversely on the magnetic field. Consequently, a stronger magnetic field lowers the critical energy, thereby increasing the conversion probability.

In contrast, the dependence of the critical energy on the mass is quadratic. Thus, as the mass increases, the critical energy required to observe conversions grows as the square of the mass. For instance, consider a candidate with $g_{a\gamma} = 8 \times 10^{-12} \text{ GeV}^{-1}$, $m_a = 2 \times 10^{-7} \text{ eV}$, and a magnetic field of $1 \mu\text{G}$; in this scenario, the critical energy is approximately 120 TeV . If the magnetic field alone is raised to $3 \mu\text{G}$ for this same candidate, the critical energy drops to about 42 TeV . However, if the mass is also increased to $2 \times 10^{-6} \text{ eV}$, the critical energy climbs to nearly 4 PeV which exceeds the current observational energy range. This example underscores the distinct role of the mass, highlighting that exploring candidates with larger masses requires access to much higher energies.

Scenario	Magnetic Field (μG)	Distance (kpc)
A	1	3.2
B	3	3.2
C	3	5
D	3	8

Table 1: Values of magnetic field strength and distance used to assess the impact of the parameters on the exclusion region. The different parameters were established by taking into account the considerations presented in Section 3.

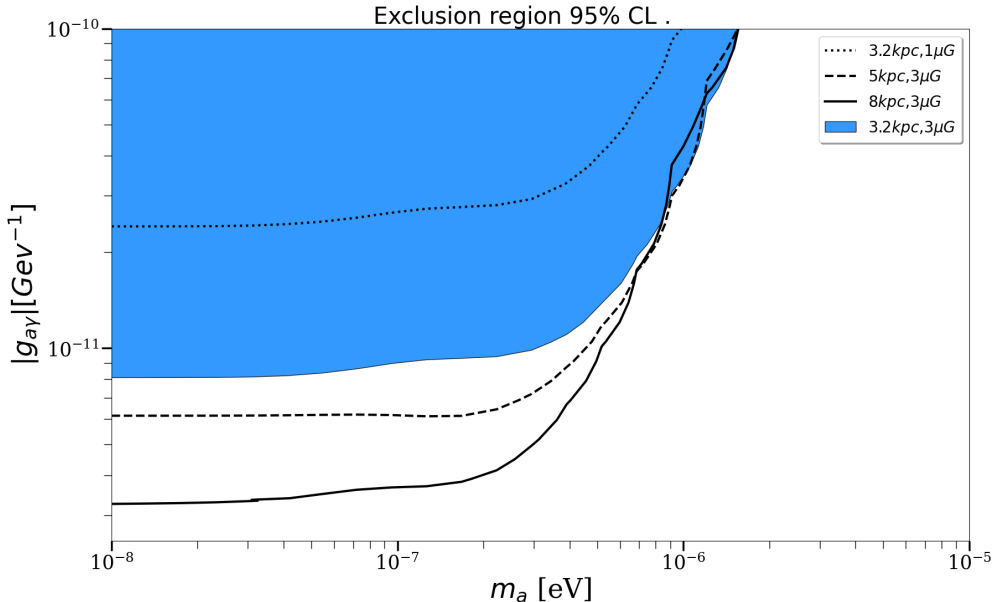


Figure 4: Comparison of exclusion regions for different values of magnetic field strength and distance to the source.

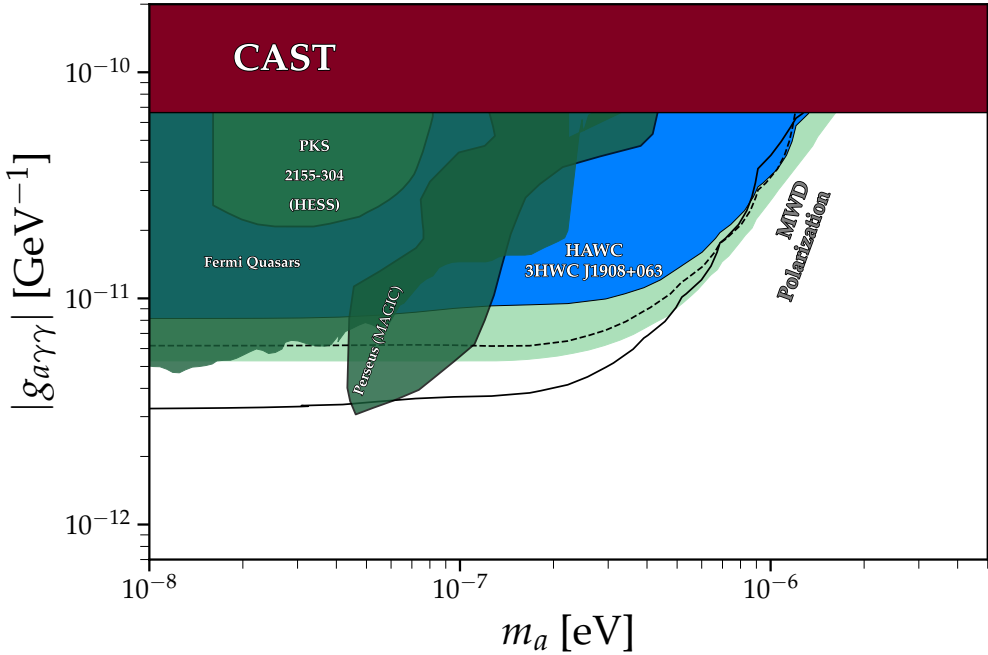


Figure 5: Exclusion regions obtained for different parameter sets are compared with existing results from various experiments, such as CAST [42], H.E.S.S[43], *Fermi*-LAT[15], [40], and measurements based on magnetic white dwarf polarization [44]. The HAWC results with baseline values of distance and magnetic field (see text) are shown as the blue shaded band. The effect of varying the distance and B-field values are shown in dashed and solid lines.

6 Conclusions

This study focused on investigating the potential impact ALPs on the UHE spectrum of the galactic source 3HWC J1908+063. We did not observe statistically significant deviations attributable to ALPs. However, the analysis enables the placement of competitive constraints on the ALP parameter space.

Exclusion regions were determined by varying key astrophysical parameters, such as magnetic field strength and distance to the source, using HAWC data. We observed that these exclusion regions expand as the magnetic field strength or distance increases. This is consistent with the fact that the conversion probability is proportional to B_T^2 and increases with the path length in the magnetic field.

Furthermore, we performed the spectral fits over an extended sky region that included not only our source 3HWC J1908+063 but also nearby sources, in order to evaluate whether the parameter values changed in any significant way. This analysis confirmed that the presence of nearby sources does not significantly impact the spectral modeling, suggesting that any potential deviations in the spectrum are more likely to be attributable to photon-ALP conversions than to contamination from nearby sources.

The constraints derived from this study contribute to the broader effort to probing the ALP parameter space and demonstrate the utility of UHE observations in setting limits on ALP properties. Future observations with more sensitive instruments and further refinement of the models could provide even tighter constraints or potentially reveal evidence of ALP-induced phenomena. In addition, it would be valuable to compare these limits with those

obtained by other observatories (see Figure 5) and methods, thereby situating them within the broader landscape of ALP searches.

Acknowledgments

We acknowledge the support from: the US National Science Foundation (NSF); the US Department of Energy Office of High-Energy Physics; the Laboratory Directed Research and Development (LDRD) program of Los Alamos National Laboratory; Consejo Nacional de Ciencia y Tecnología (CONACyT), México, grants 271051, 232656, 260378, 179588, 254964, 258865, 243290, 132197, A1-S-46288, A1-S-22784, CF-2023-I-645, cátedras 873, 1563, 341, 323, Red HAWC, México; DGAPA-UNAM grants IG101323, IN111716-3, IN111419, IA102019, IN106521, IN110621, IN110521, IN102223; VIEP-BUAP; PIFI 2012, 2013, PROFOCIE 2014, 2015; the University of Wisconsin Alumni Research Foundation; the Institute of Geophysics, Planetary Physics, and Signatures at Los Alamos National Laboratory; Polish Science Centre grant, DEC-2017/27/B/ST9/02272; Coordinación de la Investigación Científica de la Universidad Michoacana; Royal Society - Newton Advanced Fellowship 180385; Generalitat Valenciana, grant CIDEgent/2018/034; The Program Management Unit for Human Resources & Institutional Development, Research and Innovation, NXPO (grant number

References

- [1] R.D. Peccei and H.R. Quinn, [Constraints imposed by CP conservation in the presence of pseudoparticles](#), [Phys. Rev. D](#) **16** (1977) 1791.
- [2] G. Raffelt and L. Stodolsky, [Mixing of the photon with low-mass particles](#), [Physical Review D](#) **37** (1988) 1237.
- [3] J. chan Hwang and H. Noh, [Axion as a cold dark matter candidate](#), [Physics Letters B](#) **680** (2009) 1.
- [4] M. Bauer, [Yet Another Introduction to Dark Matter \[E-Book\] : The Particle Physics Approach](#), Lecture Notes in Physics ;, Springer, Cham, 1st edition 2019. ed. (2019).
- [5] S. Weinberg, [A new light boson?](#), [Phys. Rev. Lett.](#) **40** (1978) 223.
- [6] F. Wilczek, [Problem of strong \$p\$ and \$t\$ invariance in the presence of instantons](#), [Phys. Rev. Lett.](#) **40** (1978) 279.
- [7] A. Mirizzi and D. Montanino, [Stochastic conversions of TeV photons into axion-like particles in extragalactic magnetic fields](#), [Journal of Cosmology and Astroparticle Physics](#) **2009** (2017) 004.
- [8] L. Abbott and P. Sikivie, [A cosmological bound on the invisible axion](#), [Physics Letters B](#) **120** (1983) 133.
- [9] D.J. Marsh, [Axion cosmology](#), [Physics Reports](#) **643** (2016) 1.
- [10] P. Sikivie, [Experimental tests of the "invisible" axion](#), [Phys. Rev. Lett.](#) **51** (1983) 1415.
- [11] A. De Angelis, G. Galanti and M. Roncadelli, [Relevance of axionlike particles for very-high-energy astrophysics](#), [Phys. Rev. D](#) **84** (2011) 105030.
- [12] G. Galanti, F. Tavecchio, M. Roncadelli and C. Evoli, [Blazar VHE spectral alterations induced by photon-ALP oscillations](#), [Mon. Not. Roy. Astron. Soc.](#) **487** (2019) 123 [[1811.03548](#)].

[13] A. De Angelis, M. Roncadelli and O. Mansutti, Evidence for a new light spin-zero boson from cosmological gamma-ray propagation?, [Phys. Rev. D **76** \(2007\) 121301 \[0707.4312\]](#).

[14] D. Hooper and P.D. Serpico, Detecting axionlike particles with gamma ray telescopes, [Phys. Rev. Lett. **99** \(2007\) 231102](#).

[15] THE FERMI-LAT COLLABORATION collaboration, Search for spectral irregularities due to photon–axionlike-particle oscillations with the fermi large area telescope, [Phys. Rev. Lett. **116** \(2016\) 161101](#).

[16] J.-G. Guo, H.-J. Li, X.-J. Bi, S.-J. Lin and P.-F. Yin, Implications of axion-like particles from the fermi-lat and h.e.s.s. observations of pg 1553+113 and pks 2155-304, [Chinese Physics C **45** \(2021\) 025105](#).

[17] S. Jacobsen, T. Linden and K. Freese, Constraining axion-like particles with hawc observations of tev blazars, [Journal of Cosmology and Astroparticle Physics **2023** \(2023\) 009](#).

[18] A. De Angelis, O. Mansutti and M. Roncadelli, Axion-like particles, cosmic magnetic fields and gamma-ray astrophysics, [Physics Letters B **659** \(2008\) 847](#).

[19] Z. Cao and F. Aharonian, Ultrahigh-energy photons up to 1.4 petaelectronvolts from 12 γ -ray Galactic sources, [Nature **594** \(2021\) 33](#).

[20] A. Abeysekara, A. Albert, R. Alfaro, J. Angeles Camacho, J. Arteaga-Velázquez, K. Arumbabu et al., Multiple galactic sources with emission above 56 tev detected by hawc, [Physical Review Letters **124** \(2020\) .](#)

[21] Y.-F. Liang, C. Zhang, Z.-Q. Xia, L. Feng, Q. Yuan and Y.-Z. Fan, Constraints on axion-like particle properties with tev gamma-ray observations of galactic sources, [Journal of Cosmology and Astroparticle Physics **2019** \(2019\) 042](#).

[22] B.-Y. Zhu, X. Huang and P.-F. Yin, Constraints on axion-like particles from the gamma-ray observation of the galactic center, [Journal of Cosmology and Astroparticle Physics **2025** \(2025\) 030](#).

[23] C. Eckner and F. Calore, First constraints on axionlike particles from galactic sub-pev gamma rays, [Phys. Rev. D **106** \(2022\) 083020](#).

[24] J. Li, X.-J. Bi, L.-Q. Gao, X. Huang, R.-M. Yao and P.-F. Yin, Constraints on axion-like particles from the observation of galactic sources by the lhaaso*, [Chinese Physics C **48** \(2024\) 065107](#).

[25] A. Abeysekara, A. Albert, R. Alfaro, C. Alvarez, J. Álvarez, M. Araya et al., The high-altitude water cherenkov (hawc) observatory in méxico: The primary detector, [Nuclear Instruments and Methods in Physics Research Section A: Accelerators, Spectrometers, Detectors and Associated Equipment **1052** \(2023\) 168253](#).

[26] A. Albert, R. Alfaro, C. Alvarez, A. Andrés, J.C. Arteaga-Velázquez, D. Avila Rojas et al., Performance of the hawc observatory and tev gamma-ray measurements of the crab nebula with improved extensive air shower reconstruction algorithms, [The Astrophysical Journal **972** \(2024\) 144](#).

[27] A. Albert, R. Alfaro, C. Alvarez, J. Arteaga-Velázquez, D. Avila Rojas, H. Ayala Solares et al., An optimized search for dark matter in the galactic halo with hawc, [Journal of Cosmology and Astroparticle Physics **2023** \(2023\) 038](#).

[28] A. Abeysekara, A. Albert, R. Alfaro, C. Alvarez, R. Arceo, J. Arteaga-Velázquez et al., Searching for dark matter sub-structure with hawc, [Journal of Cosmology and Astroparticle Physics **2019** \(2019\) 022](#).

[29] HAWC COLLABORATION collaboration, Search for decaying dark matter in the virgo cluster of galaxies with hawc, [Phys. Rev. D **109** \(2024\) 043034](#).

[30] R. Alfaro, C. Alvarez, J.C. Arteaga-Velázquez, D.A. Rojas, H.A.A. Solares, R. Babu et al., Searching for tev dark matter in irregular dwarf galaxies with hawc observatory, [The Astrophysical Journal **945** \(2023\) 25](#).

[31] A. Albert, R. Alfaro, C. Alvarez, J.R.A. Camacho, J.C. Arteaga-Velázquez, K.P. Arunbabu et al., 3hwc: The third hawc catalog of very-high-energy gamma-ray sources, [The Astrophysical Journal **905** \(2020\) 76](#).

[32] A. Albert, R. Alfaro, C. Alvarez, J.D. Álvarez, J.R.A. Camacho, J.C. Arteaga-Velázquez et al., Hawc study of the ultra-high-energy spectrum of mgro j1908+06, [The Astrophysical Journal **928** \(2022\) 116](#).

[33] E. Aliu, S. Archambault, T. Aune, B. Behera, M. Beilicke, W. Benbow et al., Investigating the TeV Morphology of MGRO J1908+06 with VERITAS, [The Astrophysical Journal **787** \(2014\) 166](#) [[1404.7185](#)].

[34] H. E. S. S. Collaboration, H. Abdalla, A. Abramowski, F. Aharonian, F. Ait Benkhali, E.O. Angüner et al., The H.E.S.S. Galactic plane survey, [Astronomy and Astrophysic **612** \(2018\) A1](#) [[1804.02432](#)].

[35] A.A. Abdo, B. Allen, D. Berley, S. Casanova, C. Chen, D.G. Coyne et al., TeV Gamma-Ray Sources from a Survey of the Galactic Plane with Milagro, [The Astrophysical Journal **664** \(2007\) L91](#) [[0705.0707](#)].

[36] F. Aharonian, A.G. Akhperjanian, G. Anton, U. Barres de Almeida, A.R. Bazer-Bachi, Y. Becherini et al., Detection of very high energy radiation from HESS J1908+063 confirms the Milagro unidentified source MGRO, [Astronomy and Astrophysic **499** \(2009\) 723](#) [[0904.3409](#)].

[37] A. De Sarkar and N. Gupta, Exploring the hadronic origin of lhaaso j1908+0621, [The Astrophysical Journal **934** \(2022\) 118](#).

[38] R. Jansson and G.R. Farrar, A new model of the galactic magnetic field, [The Astrophysical Journal **757** \(2012\) 14](#).

[39] M. Meyer, J. Davies and J. Kuhlmann, gammaALPs: An open-source python package for computing photon-axion-like-particle oscillations in astrophysics, [PoS ICRC2021 \(2021\) 557](#) [[2108.02061](#)].

[40] H. Abe, S. Abe, J. Abhir, V. Acciari, I. Agudo, T. Aniello et al., Constraints on axion-like particles with the perseus galaxy cluster with magic, [Physics of the Dark Universe **44** \(2024\) 101425](#).

[41] H. Abdalla, H. Abe, F. Acero, A. Acharyya, R. Adam, I. Agudo et al., Sensitivity of the cherenkov telescope array for probing cosmology and fundamental physics with gamma-ray propagation, [Journal of Cosmology and Astroparticle Physics **2021** \(2021\) 048](#).

[42] V. Anastassopoulos, S. Aune, K. Barth, A. Belov, H. Bräuninger, G. Cantatore et al., New cast limit on the axion–photon interaction, [Nature Physics **13** \(2017\) 584](#).

[43] H.E.S.S. collaboration, Constraints on axionlike particles with H.E.S.S. from the irregularity of the PKS 2155-304 energy spectrum, [Phys. Rev. D **88** \(2013\) 102003](#) [[1311.3148](#)].

[44] C. Dessert, D. Dunsky and B.R. Safdi, Upper limit on the axion-photon coupling from magnetic white dwarf polarization, [Phys. Rev. D **105** \(2022\) 103034](#).